New Journal of Chemistry

Multicolored electrochromic and electrofluorochromic materials containing triphenylamine and benzoates

Wei-jing Zhang, Xin-cen Lin, Feng Li, Zhen-jie Huang, Cheng-bin Gong,* Qian Tang*

The Key Laboratory of Applied Chemistry of Chongqing Municipality, Chongqing Key Laboratory of Soft-Matter Material Chemistry and Function Manufacturing, College of Chemistry and Chemical Engineering, Southwest University, Chongqing, 400715, China. gongcbtq@swu.edu.cn, qiantang@swu.edu.cn

S1 Synthesis of compounds a-f **S2-S2**

S2 Characterization of the synthesized compounds **S3-S8**

S3 Crystal data and structure refinement **S9-S9**

S4 Cyclic voltammetry **S10-S13**

S5 Electrochromic behavior **S13-S20**

S6 Electrofluorochromic behavior of compounds 2-5 **S21-S21**

S7 DFT calculations **S22-S22**

S8 Measurement of fluorescence quantum yields **S23-S28**

S1. Synthesis of compounds a-f

Scheme S1 illustrates the synthesis of compounds **a**-**f**.

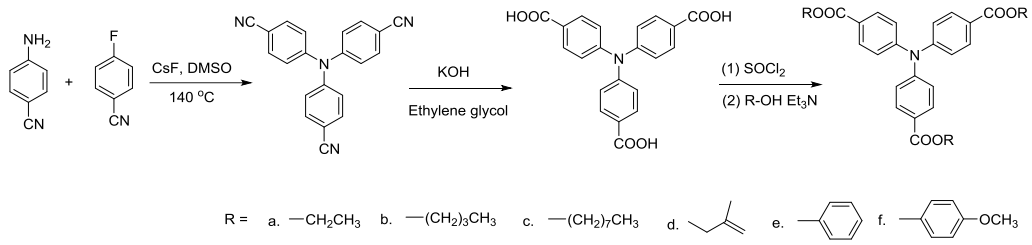

Scheme S1. Synthetic route for compounds compounds **a**-**f**.

4,4′,4″-tricyanotriphenylamine (TCTPA) was synthesized according to previous methods [1,2] with some modification. 1.18g (10 mmol) of 4-aminobenzonitrile was dissolved in 50 ml dry DMSO. then 6.04 g (40 mmol) of CsF was slowly added to the solution with continuous stirring. when 2.00 g of CsF was added the solution turned yellow and then turned green, some of the CsF was not dissolved after the all additions. And then 2.66 g (22 mmol) of 4-fluorobenzonitrile was added. After the reaction overnight, it was a brown clear solution, and the mixture was reacted at 140 ° C for 14 h. After cooling, the reaction mixture was poured into ice water to precipitate a precipitated product , which was filtered, washed with water (200 mL), ethanol (100 mL), dried, and purified by silica gel column to give 2.10 g of pure TCTPA.

4,4′,4″-nitrilotribenzoic acid (NTBA) was synthesized according to previous methods [3]. TCTPA (1.80 g, 5.62 mmol) and potassium hydroxide (1.89 g, 6 eq, 33.72 mmol) were added to a 100 mL three-neck bottle, then ethylene glycol (25 mL) was added and heated to reflux, the turbid liquid changed from white to orange-red, then turned into a brown clear and transparent solution, and the reaction was completed at 14 h. The reaction should be cooled to room temperature, 50 mL of water was added to the reaction flask, the pH was adjusted to 1 with 4 M hydrochloric acid. The reaction mixture was filtered under reduced pressure, the white solid was washed with water and dried. 2.05 g of NTBA was obtained.

4,4′,4″-nitrilotribenzoates (NTBAs) was synthesized according to previous methods [4]. The 4,4',4"-nitrilotribenzoic acid used in the synthesis of each type of ester was 2.65 mmol, and the solvent was dichloromethane.

S2. Characterization of the synthesized compounds

The prepared compounds were characterized with nuclear magnetic resonance (Bruker AV 600 (600 MHz) spectrometer) and LC/MS (Bruker impact II10200) instruments. UV-Vis spectra were collected with a UV-4802 spectrophotometer (UNICO Instruments Co. Ltd., Shanghai, China). CV was conducted using a CHI 650 B electrochemical workstation with a three-electrode system. Silver (Ag)/silver chloride (AgCl) was used as the reference electrode. A platinum disk (0.02 cm^2) and a platinum wire were used as working and counter electrodes, respectively. The CIE (International Commission on Illumination) lab color space for the ECDs based on compound **a**–**f** was measured using a color reader CR-10 plus (Konica Minolta, Inc., Japan)

(1) TCTPA

The light yellow solid was obtained by silica gel column using petroleum ether-dichloromethane (1:3, v/v) as the eluent, 2.10 g, yield: 66%. ^{1}H NMR (600 MHz, DMSO-d_6) δ (ppm): 7.81 (d, 6H, J = 9.0 Hz, Ar-H), 7.22 (d, 6H, J = 9.0 Hz, Ar-H). ^{13}C NMR (150 MHz, DMSO-d_6) δ (ppm): 149.6, 134.5, 125.5, 119.1, 106.9 [1,2].

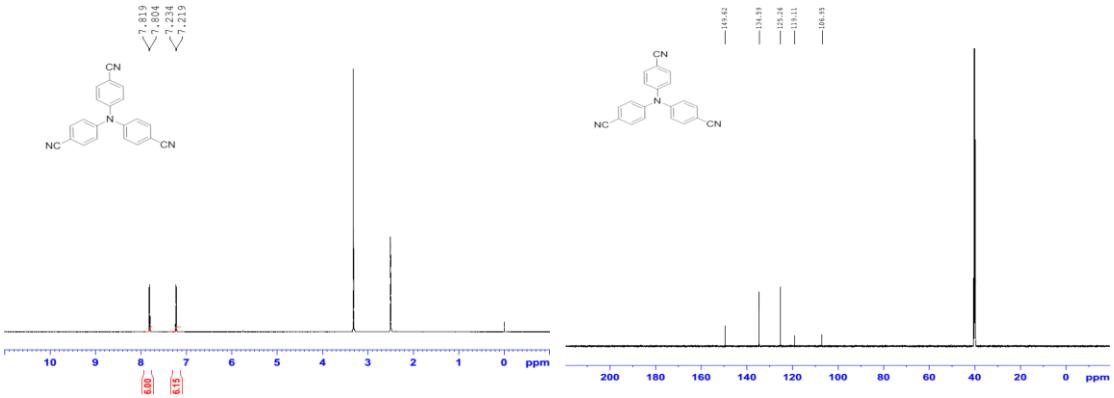

Figure. S1. ^{1}H NMR (left) and ^{13}C NMR (right) spectra of TCTPA.

(2) 4,4′,4″-Nitrilotribenzoic acid (NTBA)

White solid, 2.05 g, yield: 97%. ^{1}H NMR (600 MHz, DMSO-d_6) δ (ppm): 12.79 (s,

3H, -COOH), 7.91 (d, 6H, J = 8.4 Hz, Ar-H)，7.15 (d, 6H, J = 8.4 Hz, Ar-H). ^{13}C NMR (150 MHz, DMSO-d_6) δ (ppm): 171.9, 155.0, 136.3, 131.2, 128.9 [1,2].

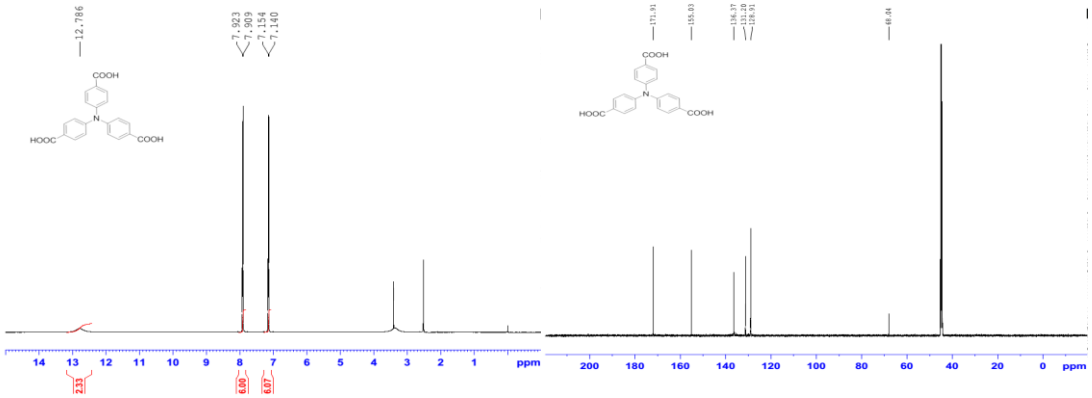

Figure S2. ^{1}H NMR (left) and ^{13}C NMR (right) spectra of NTBA.

(3) Triethyl 4,4',4"-nitrilotribenzoate (**a**)

The white solid was obtained by silica gel column chromatography using petroleum ether-dichloromethane (3:1, v/v) as the eluent, 0.96 g, yield: 79%. m.p.: 161.7-162.5 ^{o}C. ^{1}H NMR (600 MHz, $CDCl_3$) δ (ppm): 7.96 (d, 6H, J = 9.0 Hz, Ar–H), 7.12 (d, 6H, J = 8.4 Hz, Ar–H), 4.37 (m, 6H, J = 7.2 Hz, –CH_2–), 1.39 (t, 9H, J = 7.2 Hz, –CH_3). ^{13}C NMR (150 MHz, $CDCl_3$) δ (ppm): 165.9, 150.3, 131.1, 125.8, 123.7, 60.8, 14.3. HRMS (APCI): calcd for $C_{27}H_{27}NO_6$ $[M+H]^+$ 462.1911, found 462.1910.

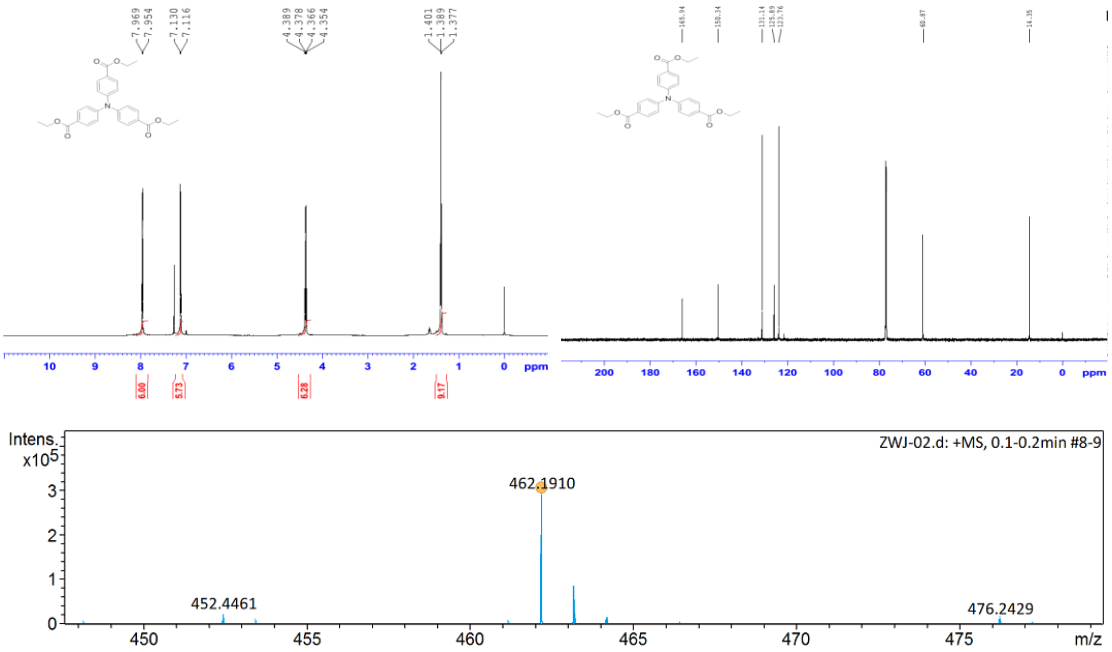

Figure S3. ^{1}H NMR (left), ^{13}C NMR (right), and mass spectra (bottom) of compound **a**.

(4) Tributyl 4,4',4''-nitrilotribenzoate (**b**)

The white solid was obtained by silica gel column chromatography using petroleum ether-dichloromethane (3:1, v/v) as the eluent, 0.68 g, yield: 47%. m.p.: 59.8-60.3 °C. ^{1}H NMR (600 MHz, $CDCl_3$) δ (ppm): 7.96 (d, 6H, J = 7.8 Hz, Ar–H), 7.12 (d, 6H, J = 7.8 Hz, Ar–H), 4.32 (t, 6H, J = 6.6 Hz, –CH_2–), 1.75 (m, 6H, J = 7.8 Hz, –CH_2–), 1.47 (m, 6H, J = 7.8 Hz, –CH_2–), 0.98 (t, 9H, J = 7.2 Hz, –CH_3). ^{13}C NMR (150 MHz, $CDCl_3$) δ (ppm): 165.9, 150.3, 131.1, 125.9, 123.7, 64.7, 30.8, 19.2, 13.7. HRMS (APCI): calcd for $C_{33}H_{39}NO_6$ $[M+H]^+$ 546.2850, found 546.2849.

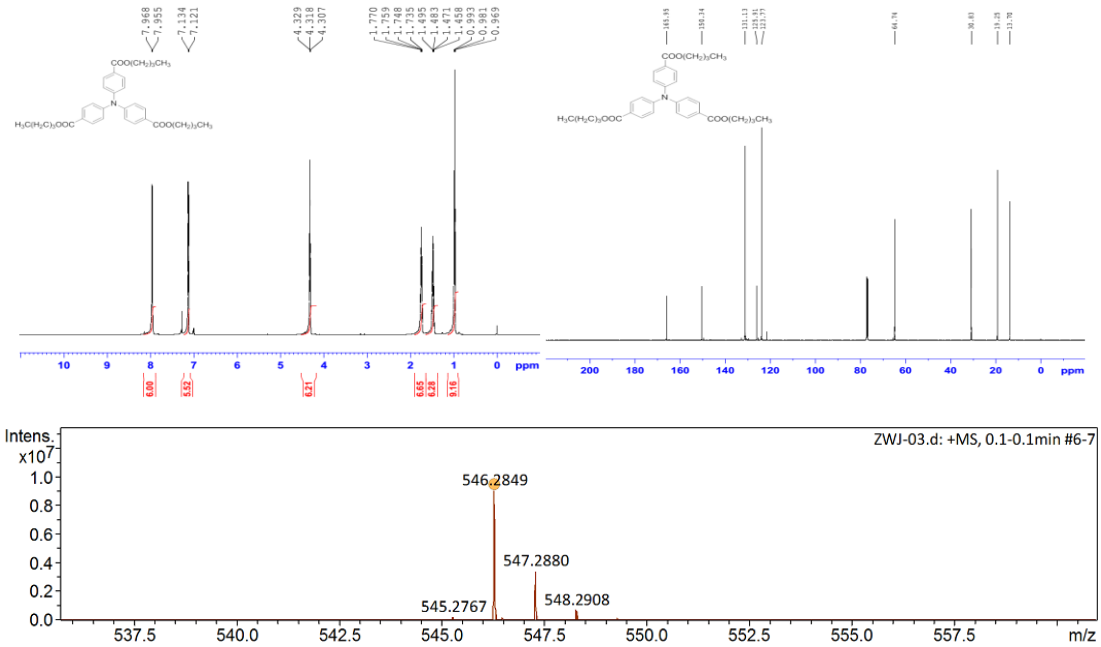

Figure S4. ^{1}H NMR (left), ^{13}C NMR (right), and mass spectra (bottom) of compound **b**.

(5) Trioctyl 4,4',4''-nitrilotribenzoate (**c**)

The light yellow oil was obtained by silica gel column chromatography using petroleum ether-dichloromethane (3:1, v/v) as the eluent, 0.82 g, yield: 44%. ^{1}H NMR (600 MHz, $CDCl_3$) δ (ppm): 7.88 (d, 6H, J = 9.0 Hz, Ar–H), 7.05 (d, 6H, J = 9.0 Hz, Ar–H), 4.23 (s, 6H, –CH_2–), 1.68 (t, 6H, J = 7.2 Hz, –CH_2–), 1.36 (t, 6H, J = 7.2 Hz, –CH_2–), 1.27 (m, 6H, –CH_2–), 1.22 (m, 18H, –CH_2–), 1.18 (t, 6H, J = 7.2 Hz, –CH_3). ^{13}C NMR (150 MHz, $CDCl_3$) δ (ppm): 166.0, 150.3, 131.1, 125.9, 123.7, 65.0, 31.7, 29.2, 29.1, 28.7, 26.0, 22.6, 14.03. HRMS (APCI): calcd for $C_{45}H_{63}NO_6$ $[M+H]^+$ 714.4728, found 741.4727.

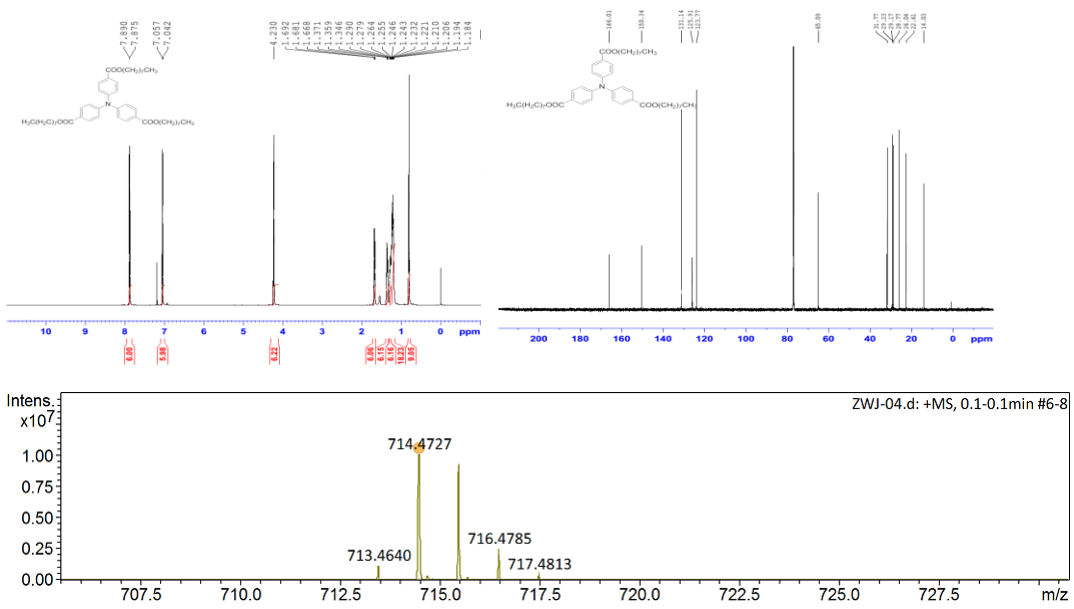

Figure S5. ^{1}H NMR (left), ^{13}C NMR (right), and mass spectra (bottom) of compound **c**.

(6) Tris(2-methylallyl) 4,4',4''-nitrilotribenzoate (**d**)

The light yellow solid was obtained by silica gel column chromatography using petroleum ether-dichloromethane (3:1, v/v) as the eluent, 0.82 g, yield: 58%. m.p.: 73.5-74.0 ºC. ^{1}H NMR (600 MHz, $CDCl_3$) δ (ppm): 7.99 (d, 6H, J = 9.0 Hz, Ar–H), 7.14 (d, 6H, J = 8.4 Hz, Ar–H), 5.07 (s, 3H, =CH_2), 4.98 (s, 3H, =CH2), 4.74 (s, 6H, –CH_2–), 1.83 (s, 9H, –CH_3). ^{13}C NMR (150 MHz, $CDCl_3$) δ (ppm): 165.5, 150.4, 140.0, 131.2, 125.6, 123.8, 112.9, 68.0, 19.5. HRMS (APCI): calcd for $C_{33}H_{33}NO_6$ $[M+H]^+$ 540.2381, found 540.2380.

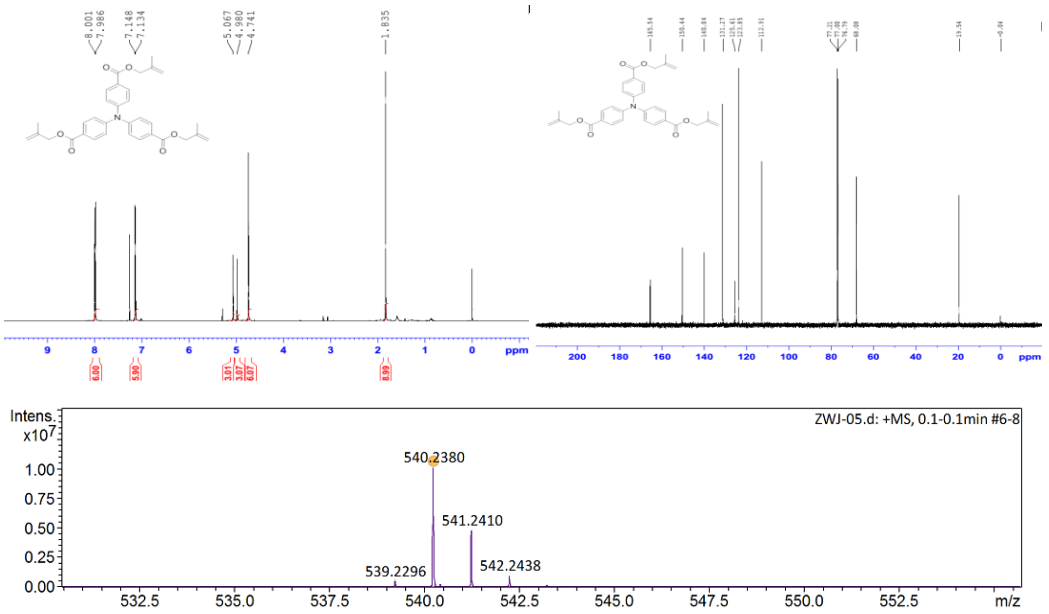

Figure S6. ^{1}H NMR (left), ^{13}C NMR (right), and mass spectra (bottom) of compound **d**.

(7) Triphenyl 4,4',4''-nitrilotribenzoate (**e**)

The white solid was obtained by silica gel column chromatography using petroleum ether-dichloromethane (3:1, v/v) as the eluent, 0.90 g, yield: 56%. m.p.: 176.5-177.5 ^{o}C. ^{1}H NMR (600 MHz, $CDCl_3$) δ (ppm): 8.17 (d, 6H, J = 9.0 Hz, Ar–H), 7.44 (t, 6H, J = 7.8 Hz, Ar–H), 7.29 (s, 6H, Ar–H), 7.26 (d, 3H, J = 7.8 Hz, Ar–H), 7.22 (d, 6H, J = 7.8 Hz, Ar–H). ^{13}C NMR (150 MHz, $CDCl_3$) δ (ppm): 164.4, 151.0, 150.8, 131.9, 129.5, 125.8, 125.1, 124.0, 121.6. HRMS (APCI): calcd for $C_{39}H_{27}NO_6$ $[M+H]^+$ 606.1911, found 606.1909.

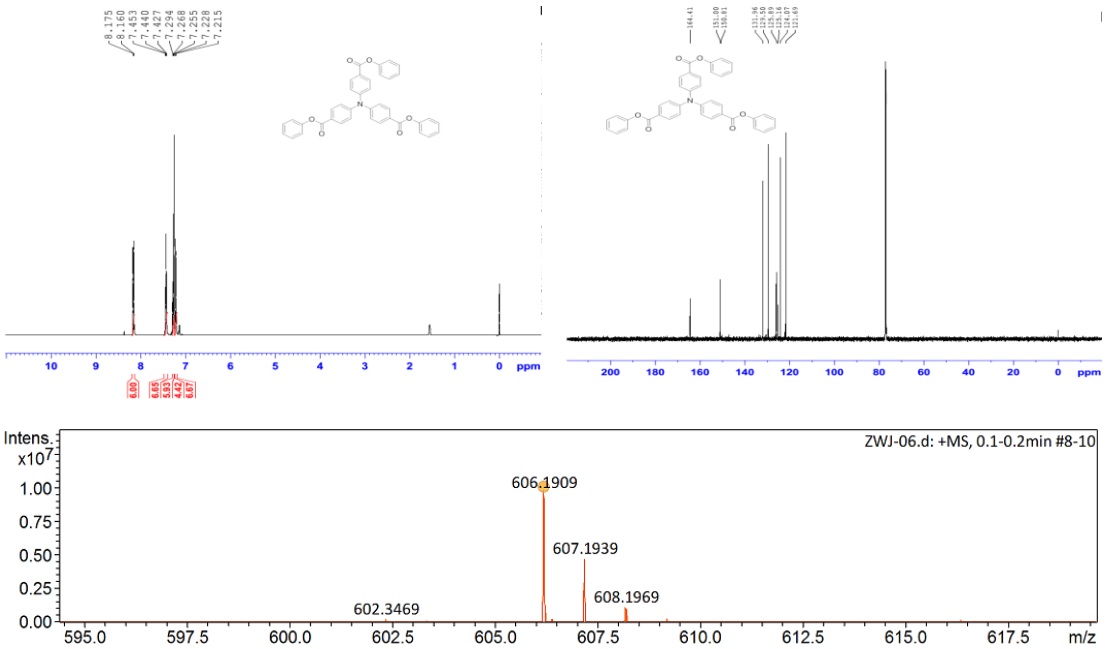

Figure S7. ^{1}H NMR (left), ^{13}C NMR (right), and mass spectra (bottom) of compound **e**

(8) Tris(4-methoxyphenyl) 4,4',4''-nitrilotribenzoate (**f**)

The white solid was obtained by silica gel column chromatography using petroleum ether-dichloromethane (3:1, v/v) as the eluent, 1.19 g, yield: 65%. m.p.: 190.0-191.4 ^{o}C. ^{1}H NMR (600 MHz, $CDCl_3$) δ (ppm): 8.14 (d, 6H, J = 8.4 Hz, Ar–H), 7.25 (d, 6H, J = 9.0 Hz, Ar–H), 7.13 (d, 6H, J = 9.0 Hz, Ar–H), 6.94 (d, 6H, J = 9.0 Hz, Ar–H), 3.83 (s, 9H, –OCH_3). ^{13}C NMR (150 MHz, $CDCl_3$) δ (ppm): 164.7, 157.3, 150.7, 144.4, 131.9, 125.3, 124.0, 122.4, 114.5, 55.6. HRMS (APCI): calcd for $C_{42}H_{33}NO_9$ $[M+H]^+$ 696.2228, found 696.2219.

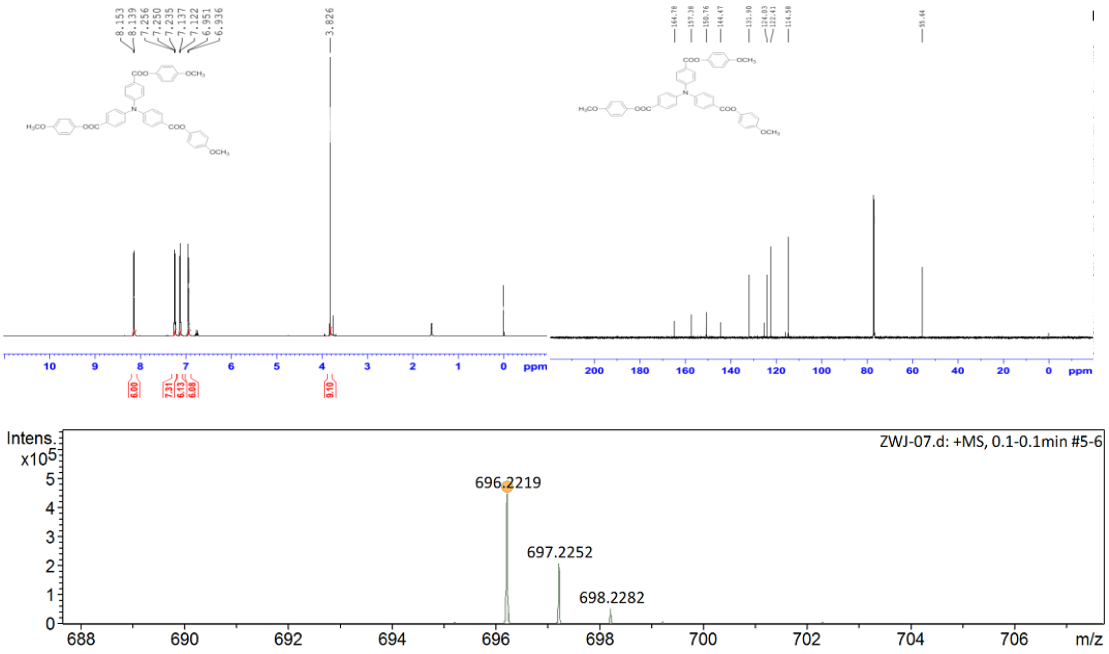

Figure S8. ^{1}H NMR (left), ^{13}C NMR (right), and mass spectra (bottom) of compound **f**.

S3. Crystal data and structure refinement

Table S1. Crystal data and experimental parameters for compound **d**

Compound	**d**
Formula	$C_{33}H_{33}NO_6$
Fw	539.60
Crystal system	orthorhombic
Space group	*P* bca
a/Å	13.68995(14)
b/Å	13.39392(17)
c/Å	31.9706(4)
α/°	90
β/°	90
γ/°	90
Volume/Å^3	5862.19(12)
Z	8
ρ_{calc} /g/cm^3	1.223
μ/mm^{-1}	0.680
radiation	CuKα
size (mm)	0.20 × 0.20 × 0.05
F(000)	2288
2θ range (deg)	8.5 to 145.994
reflns collected	22918
indep. reflns	5766 (R_{int} = 0.0305)
reflns obs. [$I > 2\sigma(I)$]	4902
data/restr/paras	5766/0/388
GOF	1.042
R1/wR2 [$I >= 2\sigma(I)$]	0.0489 / 0.1230
R1/wR2 (all data)	0.0559 / 0.1299
largest diff. peak/hole / e Å^{-3}	0.162 / -0.254
CCDC	1949105

S4. Cyclic voltammetry

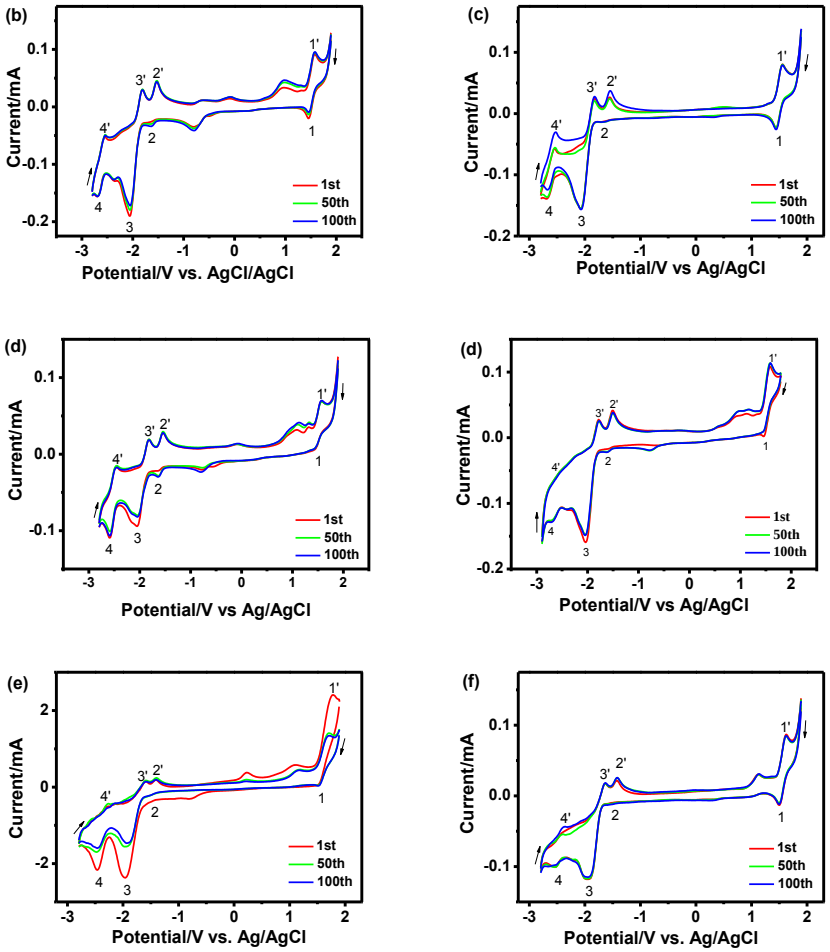

Figure S9. CV scans 100 cycles of compound **a** (A), **b** (B), **c** (C), **d** (D), **e** (E), and **f** (F) (1.0 mmol L^{-1}) in DMF/$TBAPF_6$ (50 mmol L^{-1}) vs Ag/AgCl at room temperature and a scan rate of 300 mV s^{-1}.

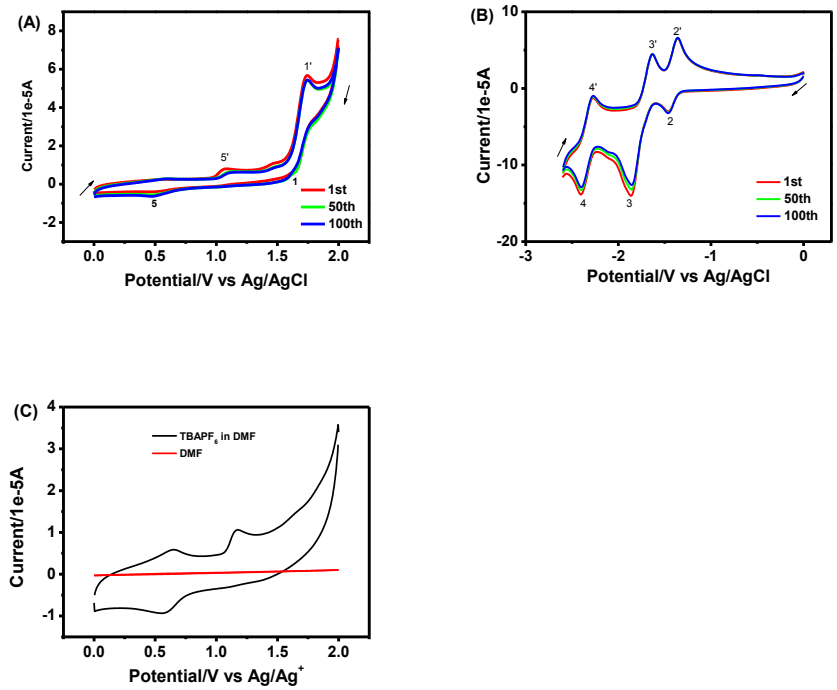

Figure S10. CV scans of compound **a** (1.0 mmol L^{-1}) in DMF/$TBAPF_6$ (50 mmol L^{-1}) between 0.0 and 2.0 V (A) and between 0.0 and -2.6 V (B) vs Ag/AgCl. CV scans of DMF and DMF/$TBAPF_6$ (50 mmol L^{-1}) (C).

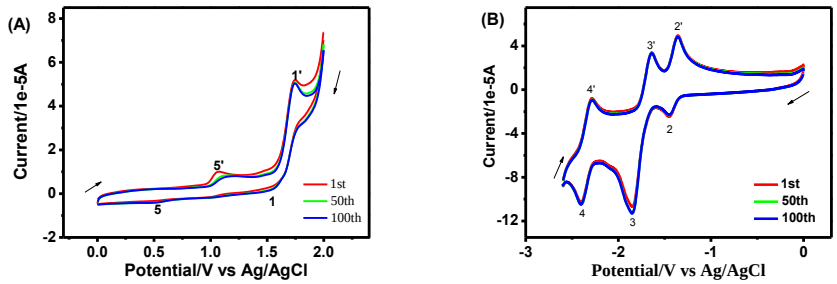

Figure S11. CV scans of compound **b** (1.0 mmol L^{-1}) in DMF/$TBAPF_6$ (50 mmol L^{-1}) between 0.0 and 2.0 V (A), and between 0.0 and -2.6 V (B) vs Ag/AgCl.

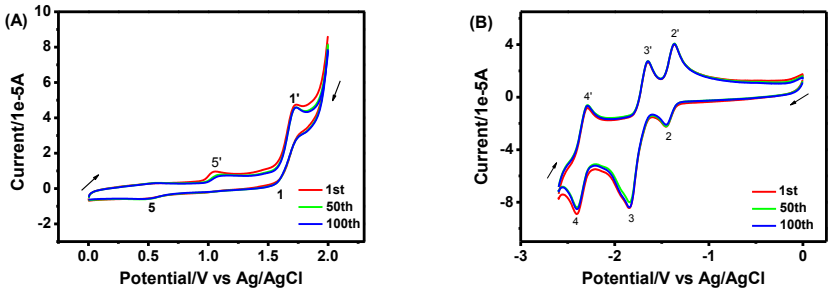

Figure S12. CV scans of compound **c** (1.0 mmol L^{-1}) in DMF/$TBAPF_6$ (50 mmol L^{-1}) between 0.0 to 2.0 V (A) and between 0.0 to -2.6 V (B) vs Ag/AgCl.

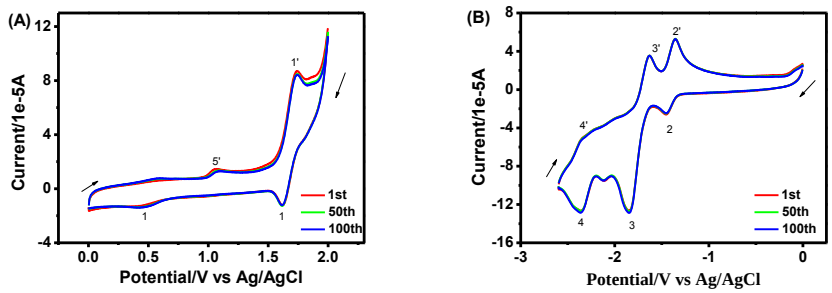

Figure S13. CV scans of compound **d** (1.0 mmol L^{-1}) in DMF/$TBAPF_6$ (50 mmol L^{-1}) between 0.0 to 2.0 V (A) and between 0.0 to -2.6 V (B) vs Ag/AgCl.

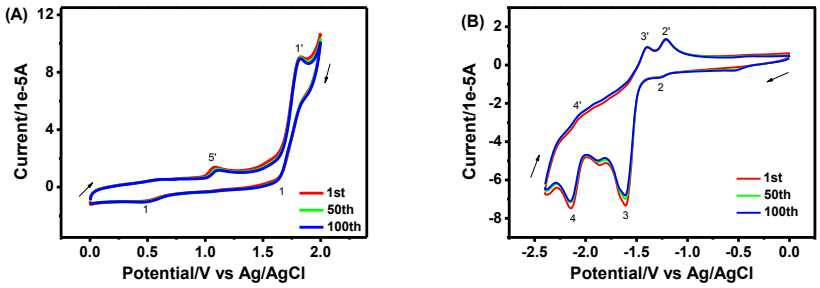

Figure S14. CV scans of compound **e** (1.0 mmol L^{-1}) in DMF/$TBAPF_6$ (50 mmol L^{-1}) at the potential between 0.0 and 2.0 V (A) and and between 0.0 to -2.4 V (B) vs Ag/AgCl.

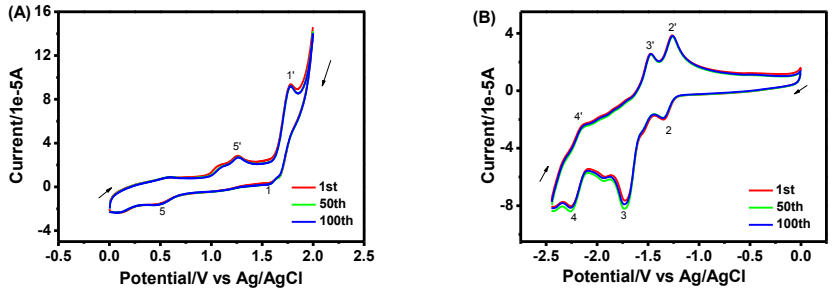

Figure S15. CV scans of compound **f** (1.0 mmol L^{-1}) in DMF/$TBAPF_6$ (50 mmol L^{-1}) at the potential between 0.0 and 2.0 V (A) and between 0.0 and -2.5 V (B) vs Ag/AgCl.

S5. Electrochromic behavior

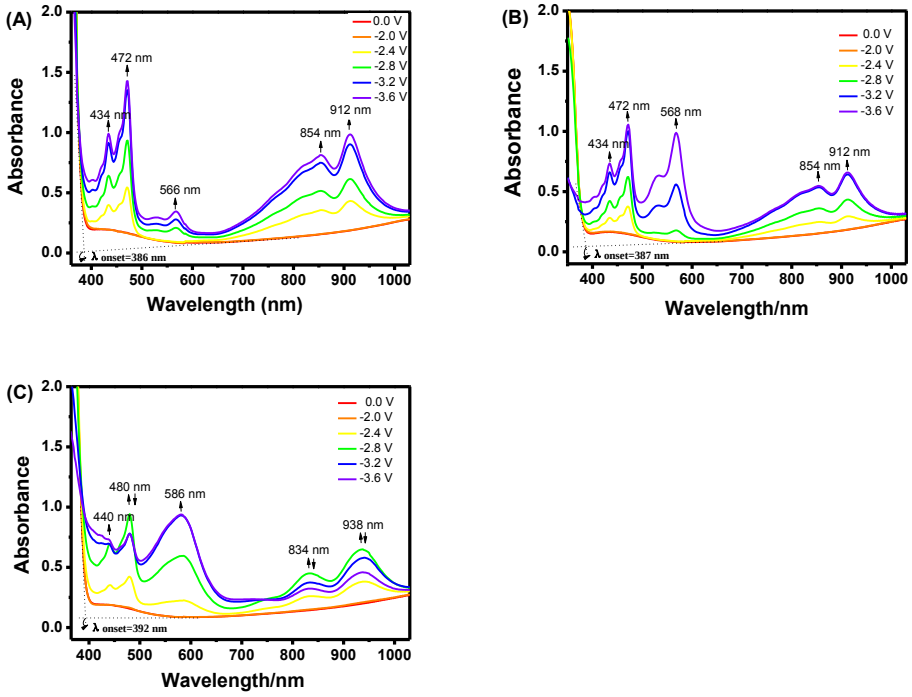

Figure S16. UV-Vis spectra of compounds **b** (A), **c** (B), and **e** (C) with a concentration of 20 mmol L^{-1} on indium tin oxide-coated glass at different potentials from -2.0 to -3.6 V.

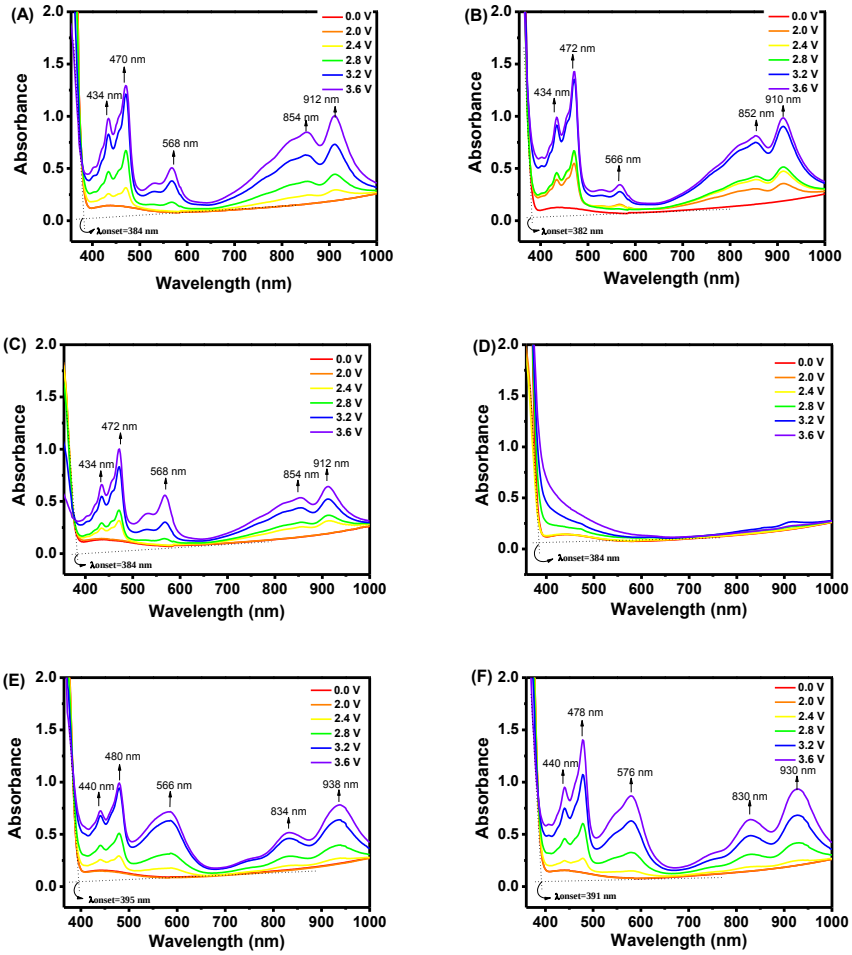

Figure S17. UV-Vis spectra of ECDs based on compound **a** (A), **b** (B), **c** (C), **c** (C), **d** (D), **e** (E), and **f** (F), with a concentration of 20 mmol/L on indium tin oxide-coated glass at different potentials from 2.0 to 3.6 V.

Figure S18. Photograph of the ECD based on compounds **b** (A), **c** (B), **d** (C), and **e** (D) in their bleached at 0.0 V and colored states at ±2.8, ±3.0, and ±3.6 V.

Table S2 The L*a*b values of compounds **a**–**f**

Compound	0.0 V			±2.8 V (**a**–**d**) ±2.6 V (**e**,**f**)			± 3.0 V			± 3.6 V		
	L	a	b	L	a	b	L	a	b	L	a	b
a	46.6	−5.4	−11.2	42.6	−8.8	2.9	39.6	−3.4	−7.9	34.2	−0.8	−9.7
b	42.5	−5.9	−12.1	40.1	−6.2	−2.6	32.7	−4.1	−6.6	34.7	−2.3	−7.4
c	45.6	−5.2	−12.0	43.0	−8.8	−4.2	38.2	−5.1	−7.9	35.4	−3.7	−8.5
d	44.8	−5.4	−10.0	41.9	−7.1	0.2	36.9	−4.2	−6.2	39.6	−2.8	−9.5
e	44.9	−5.8	−11.0	33.4	−5.6	−3.3	29.9	−4.6	−13.4	29.5	−4.7	−13.0
f	44.4	−5.7	−10.9	36.4	−5.7	−2.7	31.5	−2.9	−15.6	31.3	−3.3	−14.0

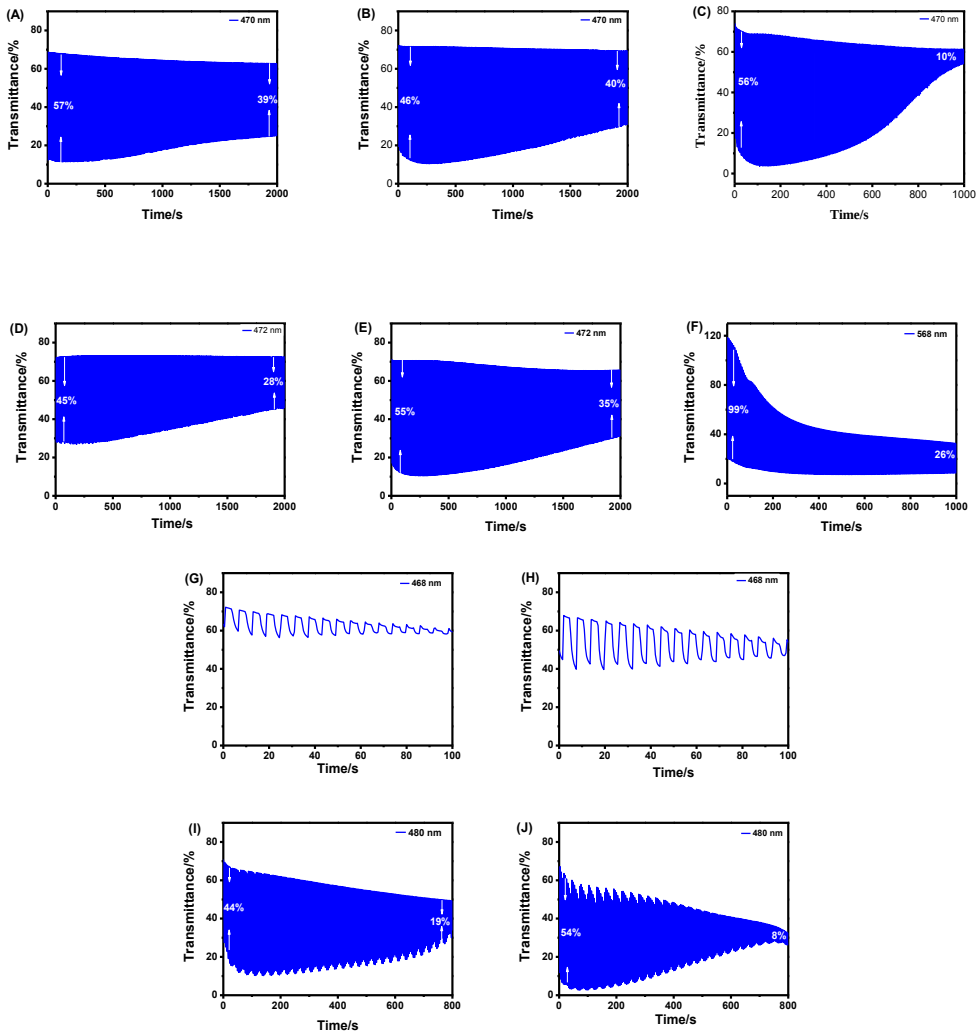

Figure S19. Optical switching behavior of electrochromic devices at 470 nm as a function of time between -2.8 V and 2.8 V (A), -3.0 V and 3.0 V (B), and -3.6 V and 3.6 V (C) for **b**, at 472 nm as a function of time between -2.8 V and 2.8 V (D) and -3.0 V and 3.0 V (E), and at 568 nm as a function of time between -3.6 V and 3.6 V (F) for **c**, at 468 nm as a function of time between -2.8 V and 2.8 V (G) and -3.0 V and 3.0 V (H) for **d**, and at 480 nm as a function of time between -2.6 V and 2.6 V (I) and -3.0 V and 3.0 V (J) for **e**, with a residence time of 4 s.

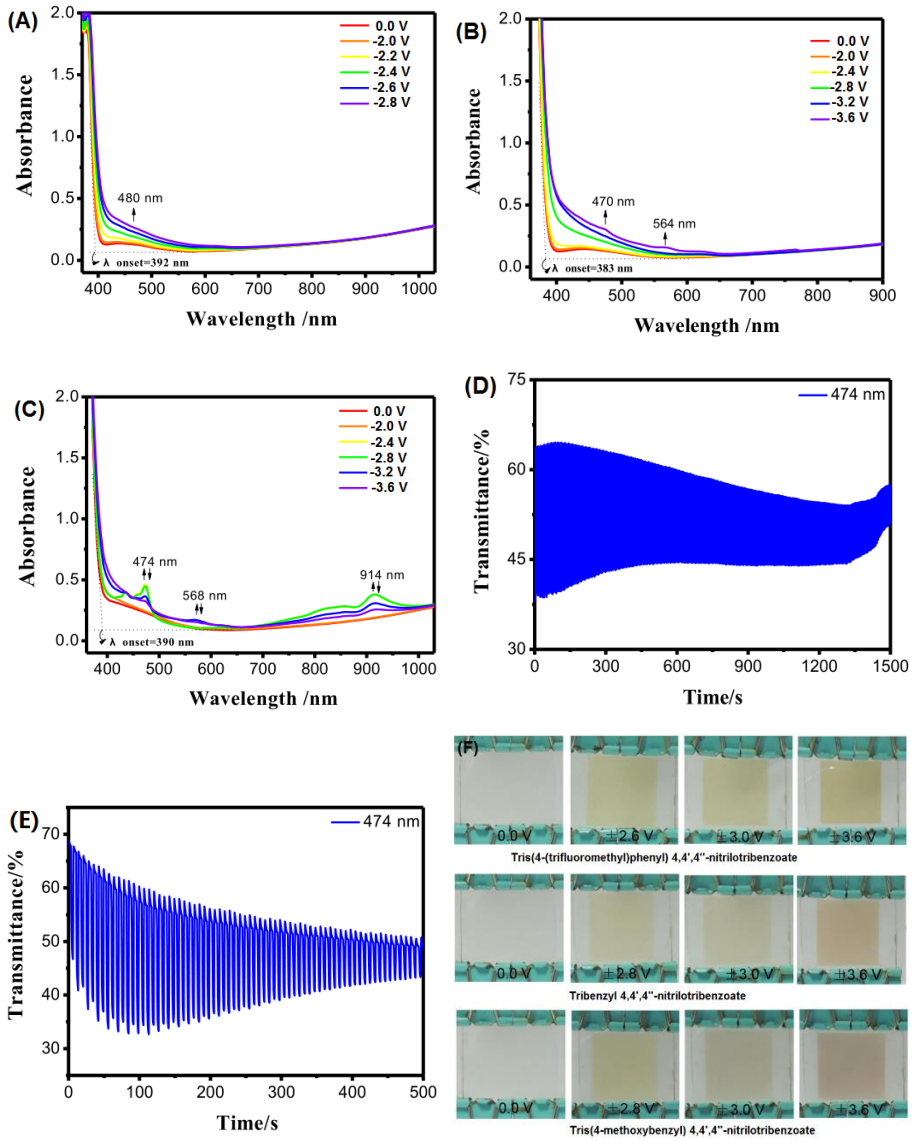

Figure S20. UV-Vis spectra of ECDs based on tris(4-(trifluoromethyl)phenyl) 4,4',4"-nitrilotribenzoate (A), tribenzyl 4,4',4"-nitrilotribenzoate (B), and tris(4-methoxybenzyl) 4,4',4"-nitrilotribenzoate (C). Optical switching behavior of ECD based on tribenzyl 4,4',4"-nitrilotribenzoate at 474 nm as a function of time between -2.8 V and 2.8 V (D), -3.0 V and 3.0 V (E). Photograph of the ECD based on tris(4-(trifluoromethyl)phenyl) 4,4',4"-nitrilotribenzoate, tribenzyl 4,4',4"-nitrilotribenzoate, and tris(4-methoxybenzyl) 4,4',4"-nitrilotribenzoate in their bleached and colored states (F).

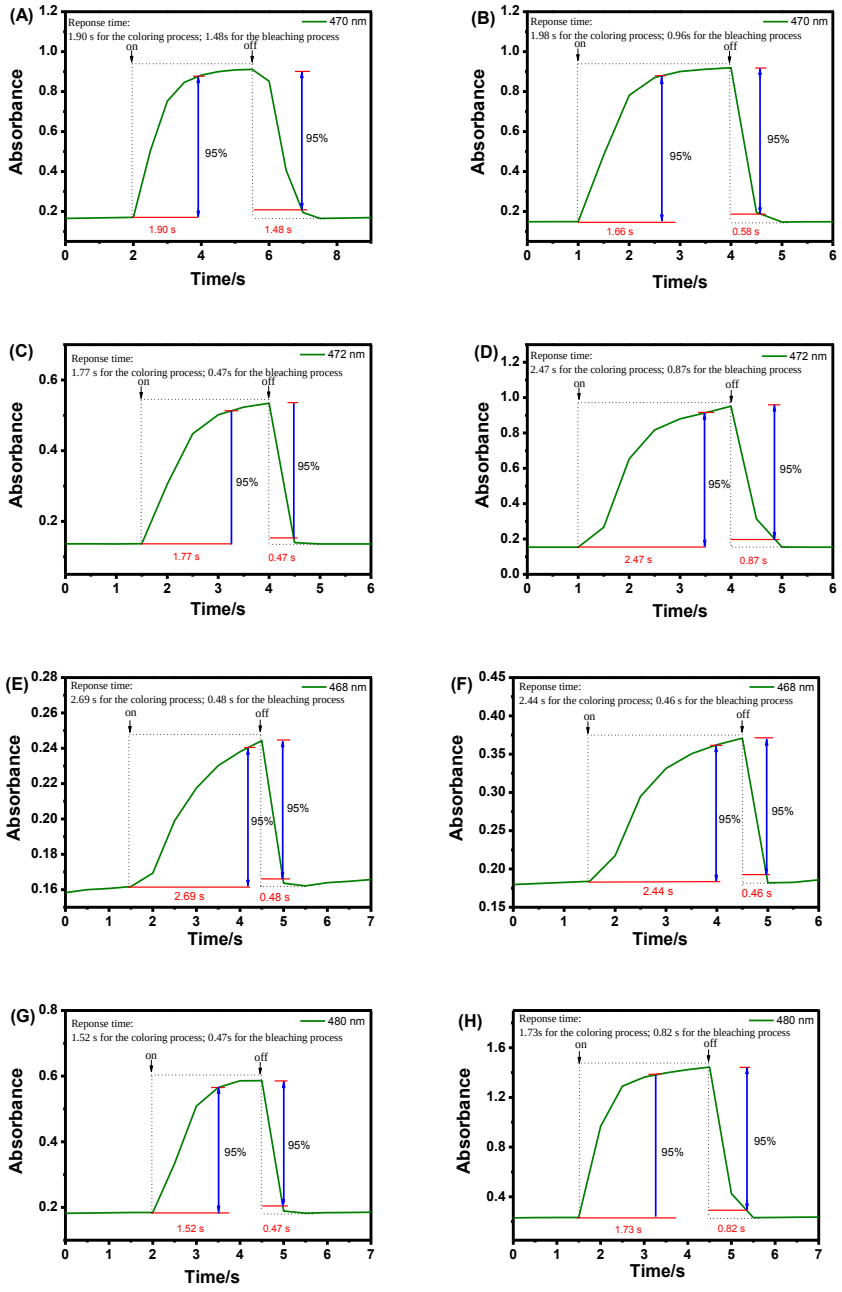

Figure S21. Electrochromic switching responses of electrochromic devices at 470 nm as a function of time between -2.8 V and 2.8 V (A) and -3.0 V and 3.0 V (B) for **b**, at 472 nm as a function of time between -2.8 V and 2.8 V (C) and -3.0 V and 3.0 V (D) for **c**, at 468 nm as a function of time between -2.8 V and 2.8 V (E) and -3.0 V and 3.0 V (F) for **d**, and at 480 nm as a function of time between -2.6 V and 2.6 V (G) and -3.0 V and 3.0 V (H) for **e** with a residence time of 4 s.

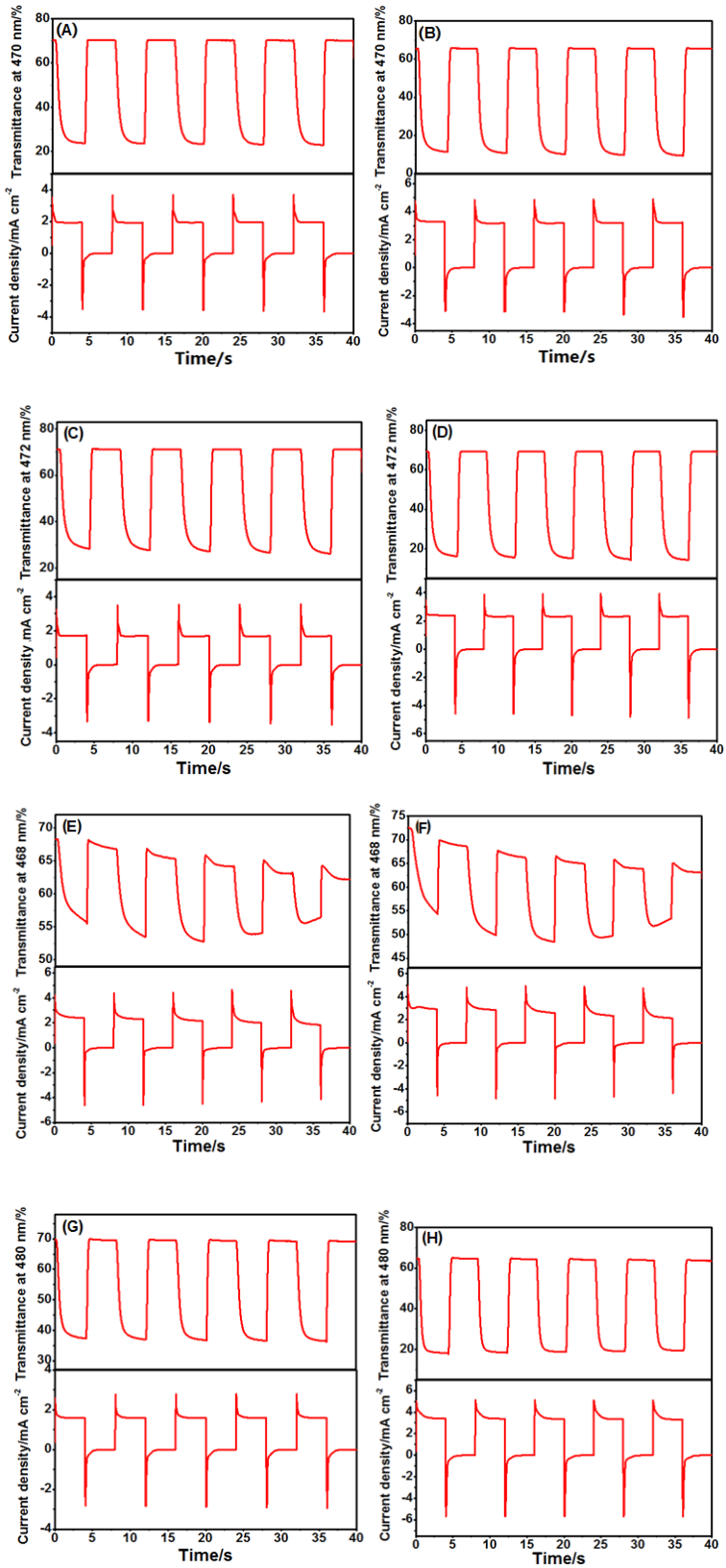

Figure S22. Chronoamperometry curve and the corresponding in-situ transmittance curve of the ECD based on compounds **b** at -2.8 V (A) and -3.0 V (B), **c** at -2.8 V (C) and -3.0 V (D), **d** at -2.8 V (E) and -3.0 V (F), and **e** at -2.6 V (G) and -3.0 V (H).

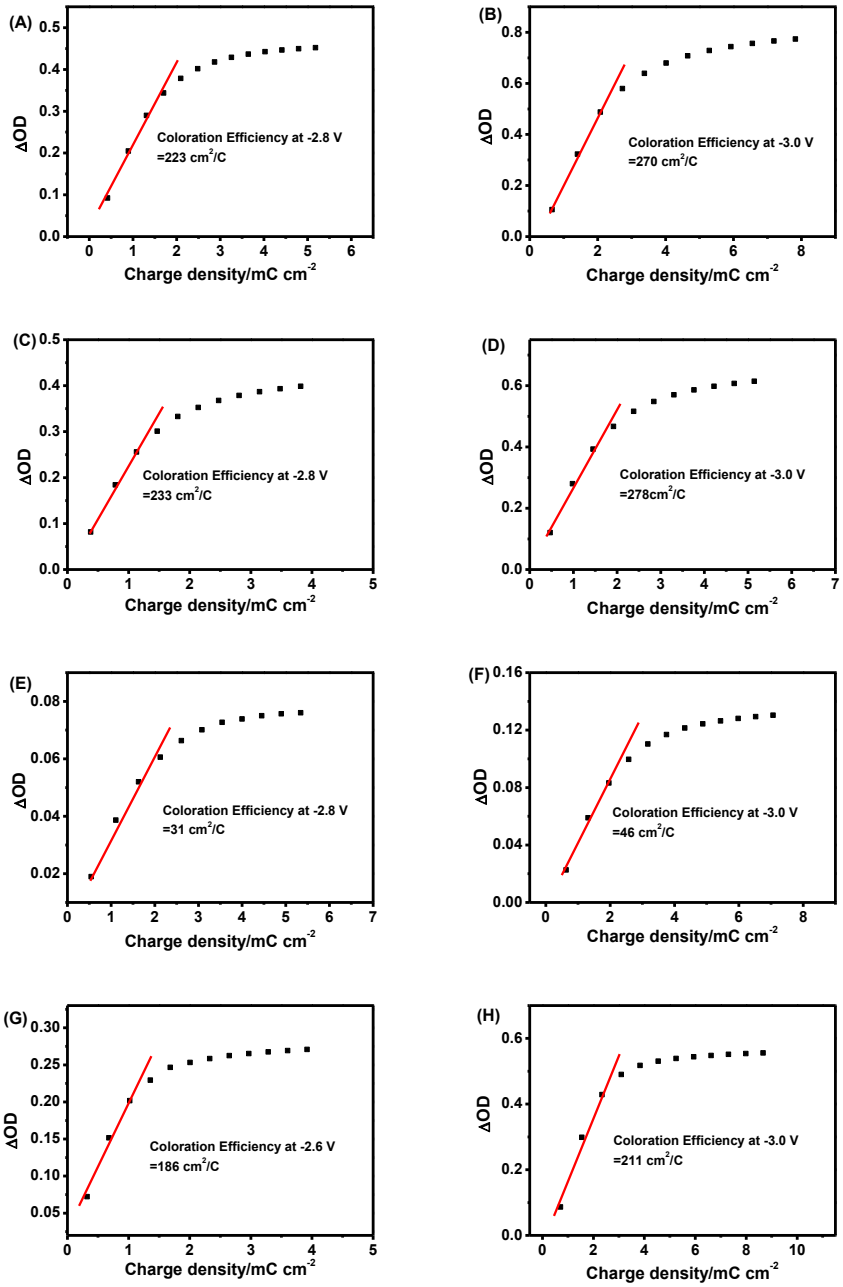

Figure S23. Optical density versus charge density of the ECD based on compounds **b** at -2.8 V (A) and -3.0 V (B), **c** at -2.8 V (C) and -3.0 V (D), **d** at -2.8 V (E) and -3.0 V (F), and **e** at -2.6 V (G) and -3.0 V (H).

S6. Electrofluorochromic behavior of compounds b-e

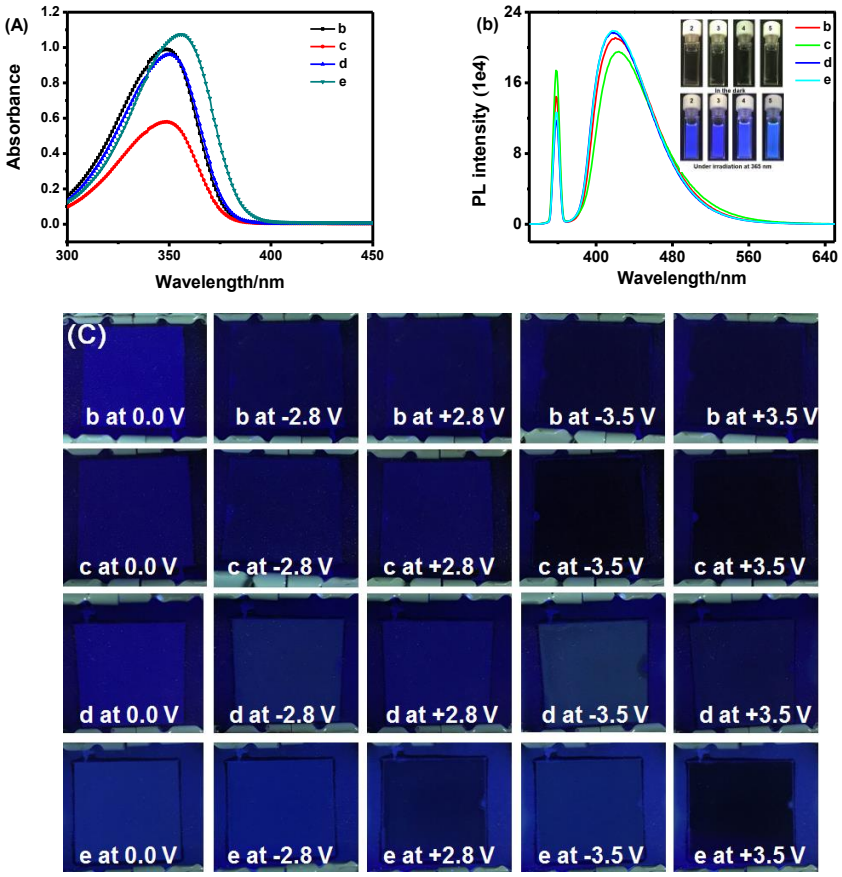

Figure S24. UV-Vis (A) and fluorescence (B) spectra of compounds **b-e** in DMF (2×10^{-5} mol/L). Photograph of the ECD based on compounds 2-5 in their bleached (0.0 V) and colored states (2.8 and 3.5 V) under irradiation at 365 nm (C). The inset photographs in (B) were taken in the dark and under illumination at 365 nm.

S7. DFT calculations

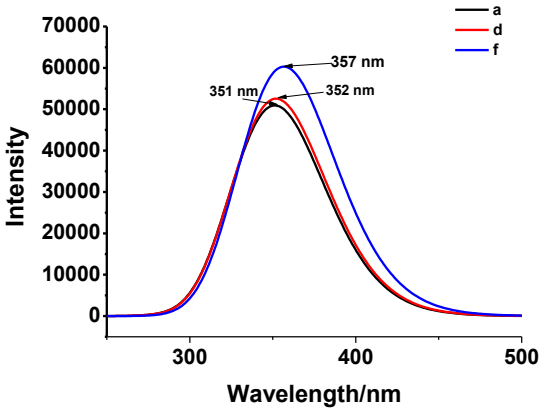

Figure S25. The simulated absorption spectra of compounds **a**, **d**, and **f**.

Table S3 The energies gap (E_{H-L}) of HOMO and LUMO, the maximum absorption peak energy (E_{ver}) of compounds **a**, **d**, and **f** in eV unit

Compounds	E_{H-L} (eV)	E_{ver} (eV)
a	3.941	3.528
d	3.934	3.522
f	3.885	3.474

Table S4 Comparison of the maximum absorption wavelength of simulated and experimental results.

Compounds	Simulated results (nm)	Experimental results (nm)
a	351	348
d	352	351
f	357	356

S8. Measurement of fluorescence quantum yields

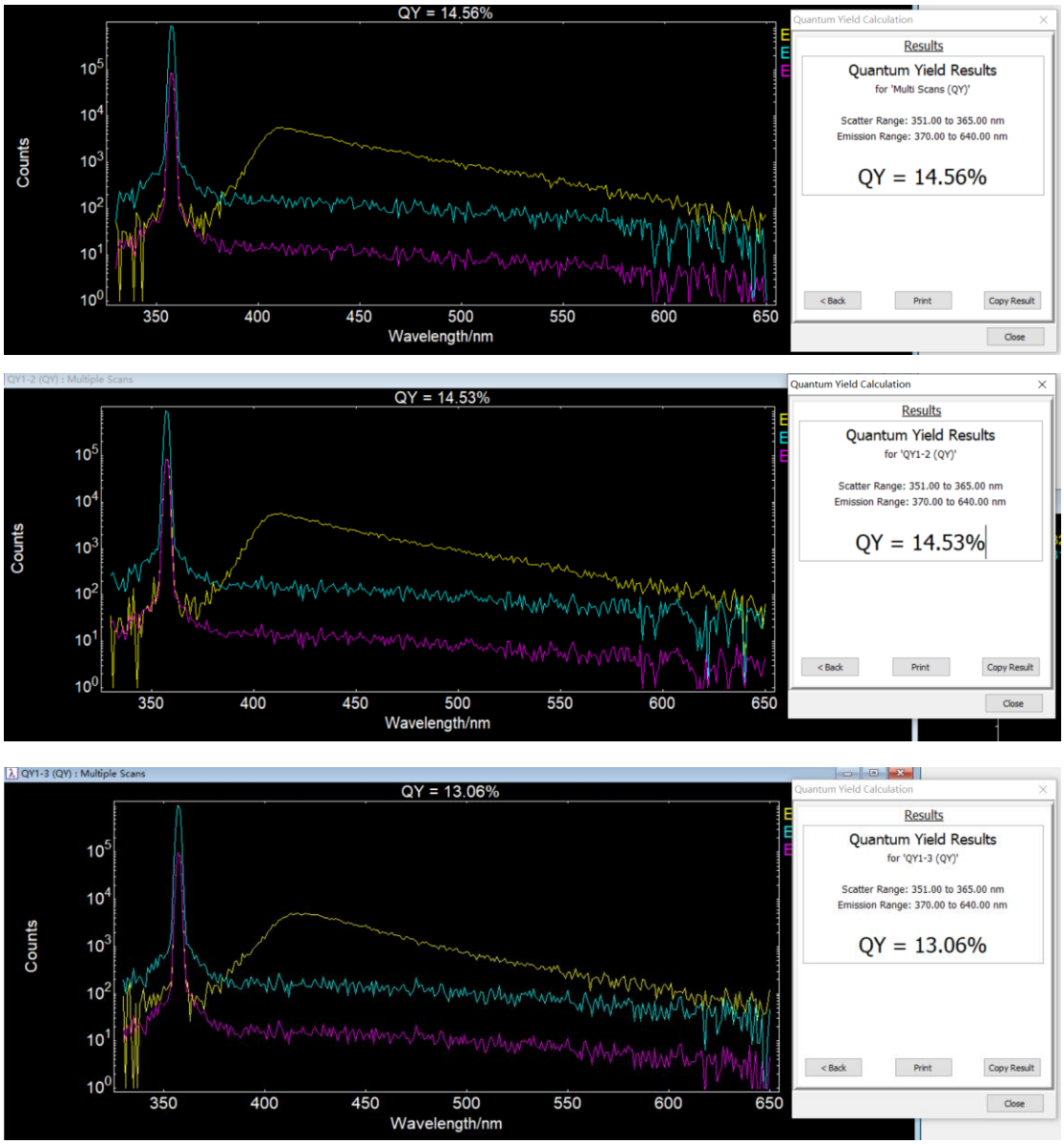

Figure S26. The fluorescence quantum yield of compound **a**.

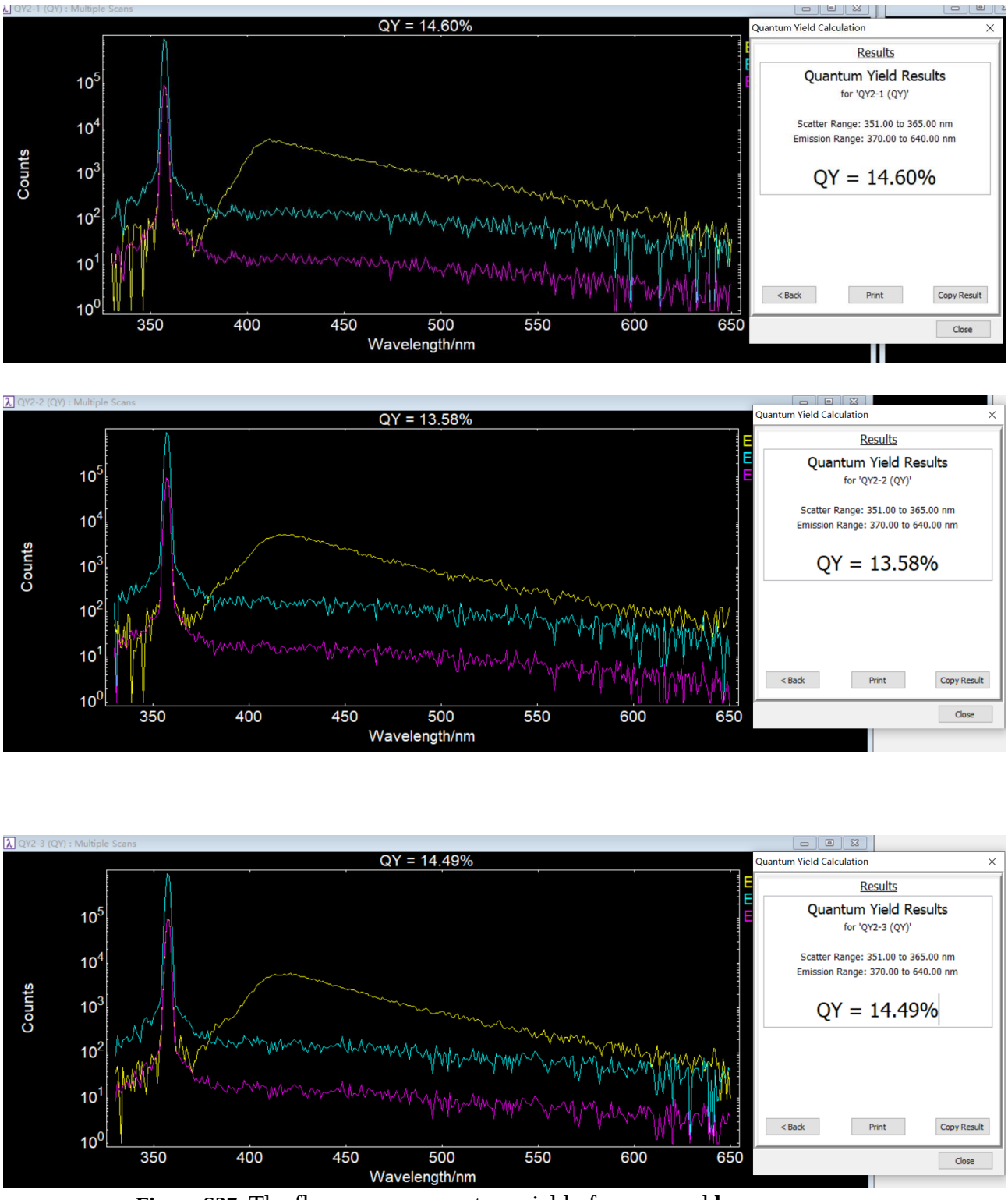

Figure S27. The fluorescence quantum yield of compound **b**.

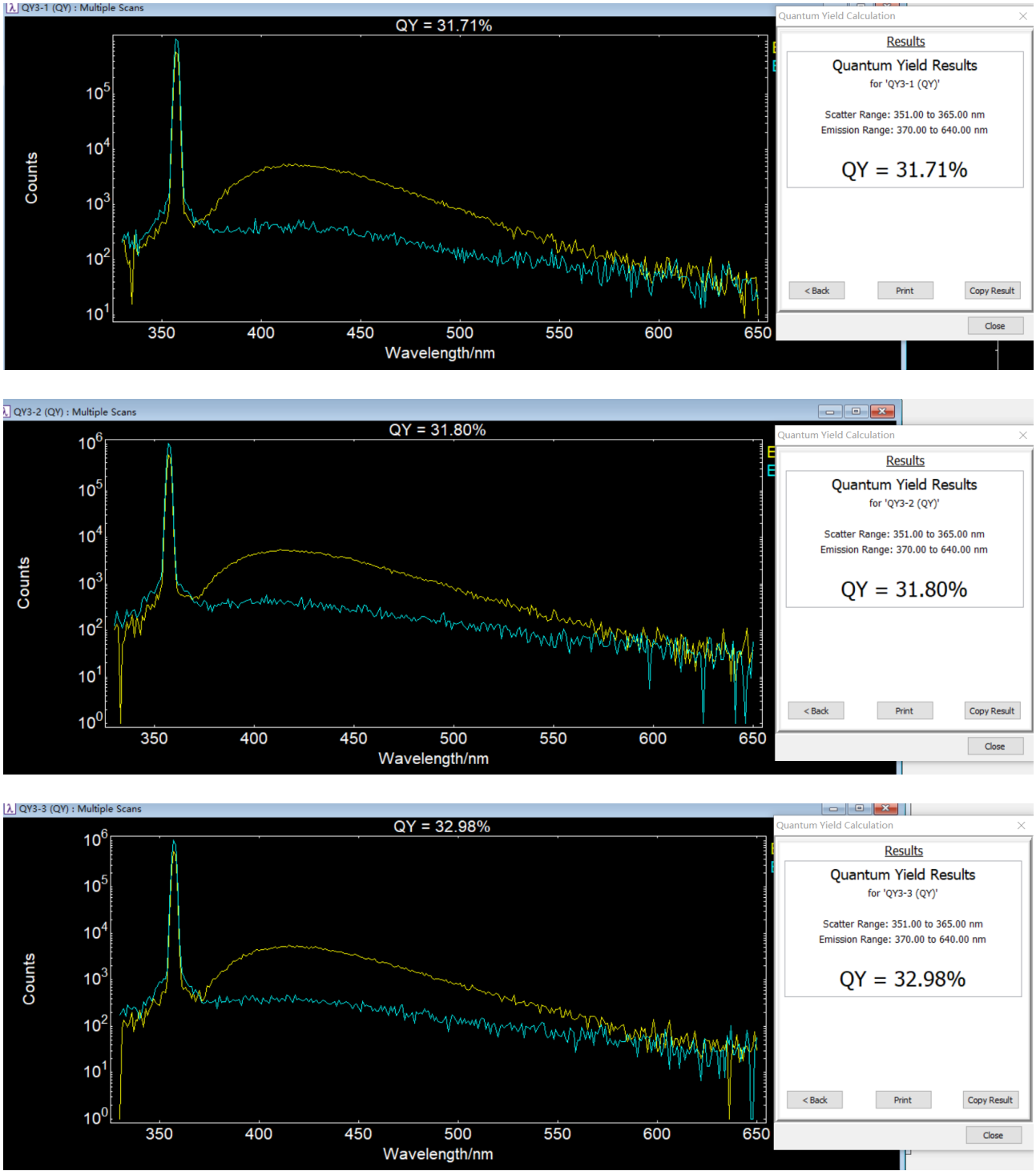

Figure S28. The fluorescence quantum yield of compound **c**.

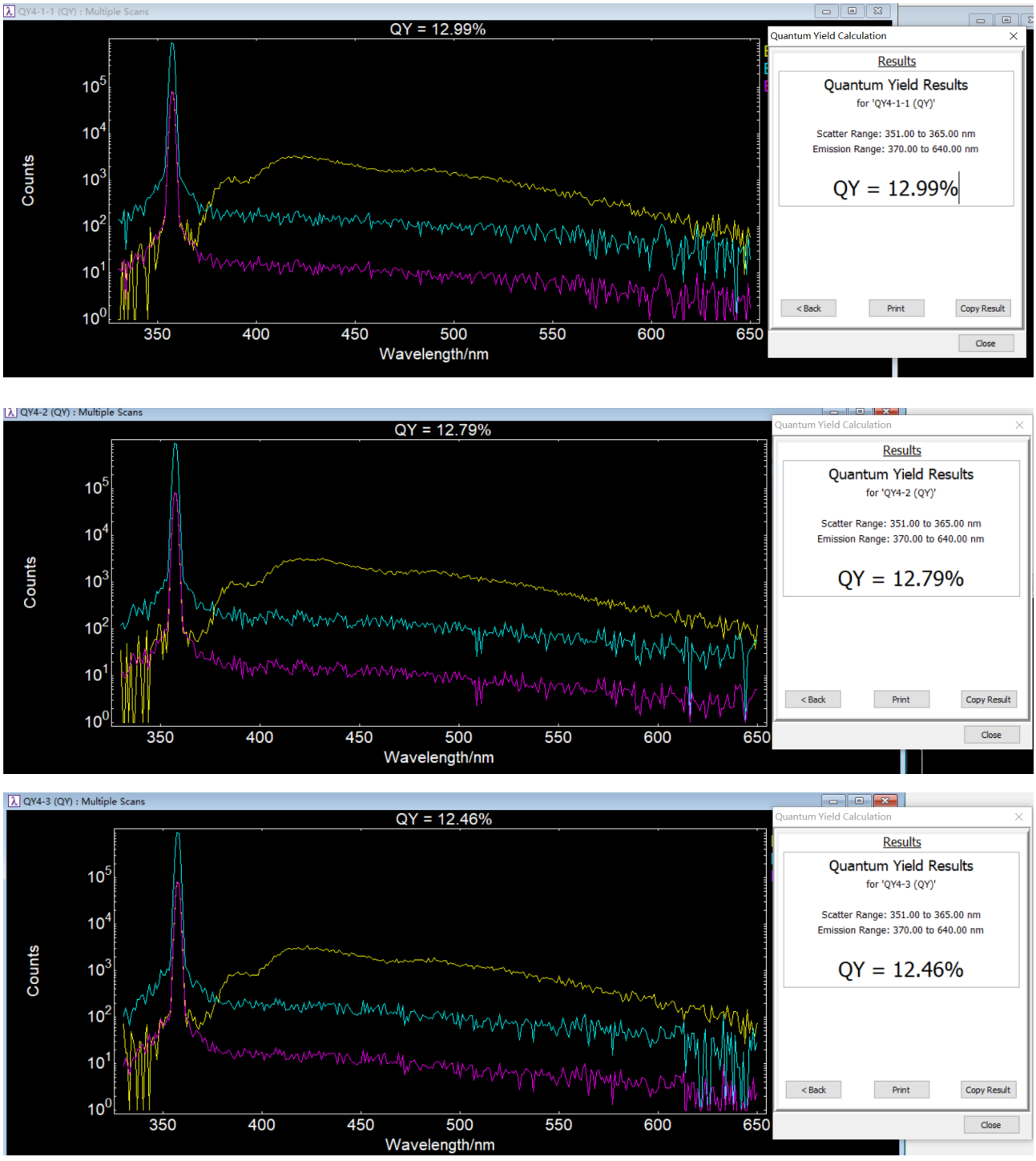

Figure S29. The fluorescence quantum yield of compound **d**.

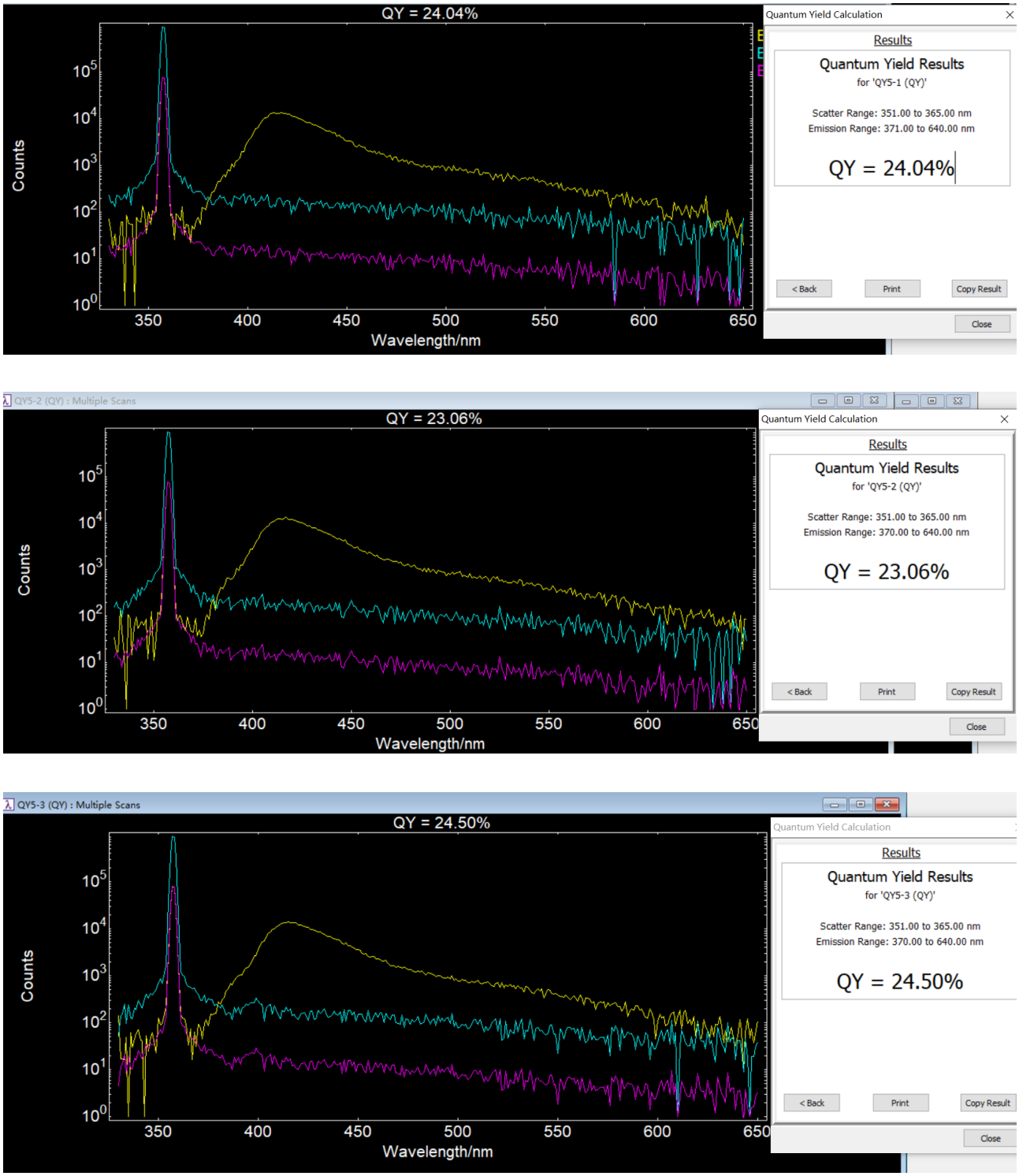

Figure S30. The fluorescence quantum yield of compound **e**.

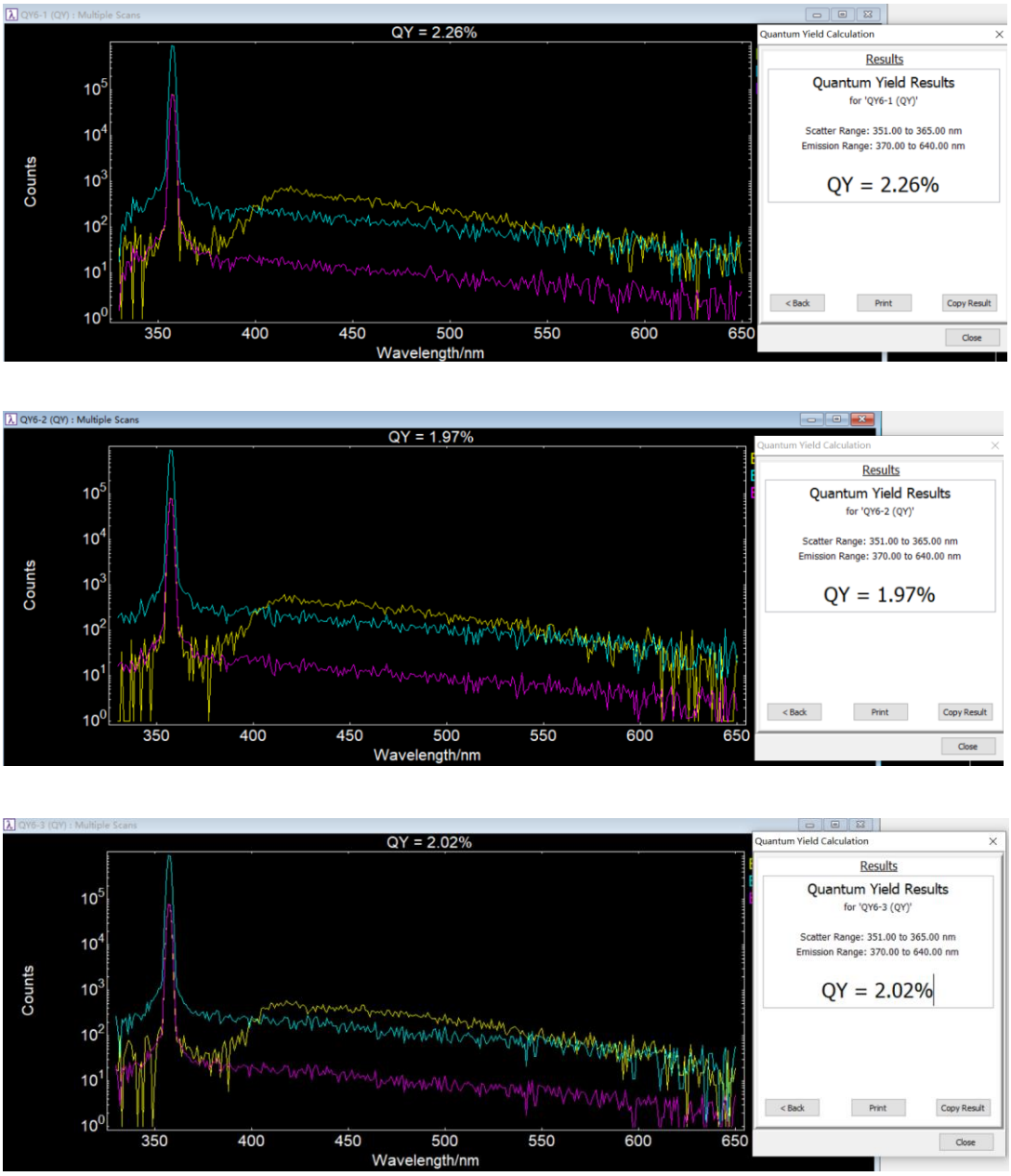

Figure S31. The fluorescence quantum yield of compound **f**.

Table S5 The fluorescence quantum yields of compounds **a-f**.

Compounds	QY1/%	QY2/%	QY3/%	$QY_{average/\%}$
a	14.56	14.53	13.06	14.05
b	14.60	13.58	14.49	14.22
c	31.71	31.80	32.98	32.16
d	12.99	12.79	12.46	12.75
e	24.04	23.06	24.50	23.87
f	2.26	1.97	2.02	2.08

References

(1) Nandi, S.; Chakraborty D.; Vaidhyanathan, R. A Permanently Porous Single Molecule H-bonded Organic Framework for Selective CO_2 Capture. *Chem. Commun.* **2016**, *52*, 7249-7252

(2) Hsiao, S. H.; Chen, Y. Z. Electrosynthesis of Redox-Active and Electrochromic Polymer Films from Triphenylamine-cored Star-shaped Molecules End-capped with Arylamine Groups. *European Polymer JournaL* **2018**, *l 99*, 422-436

(3) Chen, C. X.; Wei, Z.W.; Jiang, J. J.; Fan, Y. Z.; Zheng, S. P.; Cao, C. C.; Li, Y. H.; Fenske, D.; Su, C. Y. Precise Modulation of the Breathing Behavior and Pore Surface in Zr-MOFs by Reversible Post-Synthetic Variable-Spacer Installation to Fine-Tune the Expansion Magnitude and Sorption Properties. *Angew. Chem. Int. Ed.* **2016**, *55*, 1-6

(4) Zhang, W. J.; Zhu, C. R.; Huang, Z. J.; Gong, C. B.; Tang, Q.; Fu, X. K. Electrochromic 2,4,6-Triphenyl-1,3,5-Triazine based Esters with Electron Donor-Acceptor Structure. *Org. Electron*. **2019**, *67*, 302–310.